International Journal of Science and Research (IJSR)
ISSN: 2319-7064
Impact Factor 2025: 7.089

Biosynthesis of Zinc Oxide Nanoparticles from Microbial Source: A Sustainable and Eco-Friendly Approach

Swapnil Pradhan[1], Shravani Ramesh Wadekar[2*], Manish Shamrao Hate[3], Ramesh Chaughule[4]

[1]Research student, Department of Microbiology, Ramnarain Ruia Autonomous College, L.N. Road, Matunga (east), Mumbai- 400019, India

[2]Research Student, Department of Chemistry, Ramnarain Ruia Autonomous College, L.N. Road, Matunga (east), Mumbai- 400019, India
Corresponding Author Email: *shravaniwadekar996[at]gmail.com*

[3]Head of the Chemistry Department, Ramnarain Ruia Autonomous College, L.N. Road, Matunga (East), Mumbai-400019, India

[4]Adjunct Professor, Ramnarain Ruia Autonomous College, Mumbai-400019, India

Abstract: ***This study investigates the biosynthesis of zinc oxide nanoparticles (ZnO NPs) using Escherichia coli and Aspergillus niger through intracellular and extracellular pathways employing zinc nitrate hexahydrate as a precursor. The synthesized nanoparticles were characterized using UV-Vis spectroscopy, FTIR, FESEM, and EDAX to evaluate their optical properties, functional groups, morphology, and elemental composition. UV-Vis analysis revealed characteristic absorption peaks within the range of 310 nm to 360 nm, confirming nanoparticle formation. FTIR spectra indicated the presence of hydroxyl, amine, and carbonyl groups acting as reducing and stabilizing agents. FESEM analysis demonstrated diverse morphologies including spherical and rod-like structures, while EDAX confirmed zinc composition. Antibacterial assays showed maximum inhibition zones of up to 18 mm against Staphylococcus aureus, highlighting strong antimicrobial activity. The results demonstrate that microbial synthesis provides an eco-friendly, cost-effective, and sustainable alternative to conventional methods with potential applications in biomedical and environmental fields.***

Keywords: Green nanotechnology, Biosynthesis, Antibacterial activity, Nanomaterials Characterization, Microbial nano factories, Eco-friendly synthesis

1. Introduction

Over the last decade, nanotechnology has been applied in various domains, including medicine and chemical engineering, and has significantly advanced multiple fields. Numerous studies have investigated the production of nanoparticles from diverse sources, including physical, biological, and chemical origins. Biological sources are increasingly preferred due to their cost-effectiveness and sustainability in comparison to the other two approaches, which primarily involve high energy processes and toxic reagents. Recent advancements in nanotechnology enable the synthesis of nanoparticles of varying diameters, which can also be accomplished by microbiological sources[1]. Microorganisms, particularly bacteria and fungi, possess an inherent capacity to interact with metal salts convert metal ions into metal oxide nanoparticles, both intracellularly and extracellularly. This technique enables the use of non-toxic reagents and enables the straightforward synthesis of nanoparticles.

Microbial-derived nanoparticles demonstrate enhanced thermal, physical, chemical, and biological characteristics relative to bulk materials. Bacteria and fungi can produce nanoparticles both intracellularly and extracellularly, influenced by parameters such as growth rate, temperature, synthesis duration, and metal salt concentration[2,3]. Microorganisms act as biological nano-factories, employing reductase enzymes to transform metal ions into metal or metal oxide nanoparticles in an environmentally sustainable, economical, and non-toxic fashion; yet, limitations remain in large-scale cultivation and preservation. Among various metal oxides, zinc oxide nanoparticles (ZnO NPs) are extensively utilized in optical, piezoelectric, magnetic, and gas-sensing applications[1,2]. Zinc, a vital nutrient, facilitates microorganisms, including bacteria, yeast, and fungi, in synthesizing ZnO NPs via intracellular and extracellular processes, with reaction optimization governing nanoparticle dimensions and form[4]. Intracellular mechanisms refer to the biochemical and molecular processes that occur within a cell, regulating functions such as metabolism, signalling, gene expression, and apoptosis. In contrast, extracellular mechanisms involve processes that occur outside the cell, including cell–cell communication, interaction with the extracellular matrix, and signalling via hormones, cytokines, or growth factors.

Bacteria are recommended for nanoparticle manufacturing due to their controllability, fast growth, and ability to release enzymes and proteins that reduce zinc ions and stabilize nanoparticles[4]. Moreover, bacteria are more reproducible than plants and can serve as an alternative to plant-mediated synthesis[5]. The development of monodispersed or polydispersed nanoparticles depends on the synthesis process and medium conditions; therefore, choosing the right microbiological source is critical[5]. Although bacterial intracellular and extracellular ZnO NPs synthesis has not been fully explored, bacteria can tolerate heavy metals and influence nanoparticle production through their metabolic activities[5]. *E. coli*, a gram-negative bacterium, grows rapidly, is readily cultivable, and secretes proteins and biomolecules that reduce and stabilize nanoparticles, making it an excellent candidate for ZnO NPs synthesis[6-9]. However, the mechanism of ZnO NPs production in *E. coli* remains unclear.

The microbial synthesis of ZnO NPs occurs via two mechanisms: extracellular reduction of Zn^{2+} ions by secreted enzymes such as NADH-dependent or nitrate reductase, and intracellular synthesis through Zn^{2+} ion uptake followed by reduction in the periplasm or cytoplasm. Both pathways involve the formation of $Zn(OH)_2$ intermediates that dehydrate to generate ZnO nuclei, while proteins and peptides act as natural capping agents to stabilize the nanoparticles[7-8].

Intracellular synthesis is governed by the ionic charge of the microbial cell wall. Zinc ions interact with negatively charged functional groups such as carboxylate, phosphate, and hydroxyl groups, leading to their adsorption and uptake by the bacterial cells[4,9]. These ions are reduced by NADH through NADH- dependent reductase located in the plasma membrane, resulting in ZnO NPs formation within the periplasmic space or cytoplasm. The nanoparticles are subsequently capped and stabilized by intracellular biomolecules[4].

Fungi, on the other hand, act as efficient bio-factories as they secrete enzymes, proteins, and secondary metabolites that function as reducing and stabilizing agents during nanoparticle synthesis[10]. Although time-consuming, fungal ZnO NPs production is straightforward, cost-effective, and environmentally friendly. Fungi are often preferred over bacteria due to their higher enzyme production, ease of handling, and adherence to green chemistry principles[10]. Their filamentous mycelial network enhances metal binding and nanoparticle nucleation due to a high surface area and abundant functional groups[11]. Consequently, fungi represent a viable and sustainable biological source for large-scale, green synthesis of zinc oxide nanoparticles, owing to their unique structural and biochemical properties[11].

In this study, a comparative evaluation of pellet- and supernatant-mediated synthesis was carried out to investigate their respective roles in the synthesis process.

2. Materials and Methodology

Procurement and culturing of *Escherichia coli (E. coli*) and *Aspergillus niger* (*A. niger*):
Strains of *E. coli* and *A. niger* were procured from National Centre for Cell Science (NCCS), Pune. The bacterial strain (*E. coli*) was subcultured in Nutrient Broth (Himedia-M002), whereas the fungal strain (*A. niger*) was grown in Potato Dextrose Broth (Himedia-GM403). A loopful from each culture was aseptically introduced into sterile broth with a sterile inoculating needle. The inoculated Nutrient Broth was incubated at 37 °C for 24 hours, whereas the Potato Dextrose Broth was incubated at 30 °C for 72 hours. Following incubation, the observation of turbidity verified microbial proliferation. The cultures were subsequently preserved at low temperatures for future experimental use.

All chemicals were of A.R. grade with 100 percent purity. Zinc Nitrate Hexahydrate ($Zn(NO_3)_2 \cdot 6H_2O$) and acetone (for sterilization purpose) were obtained from LOBA CHEMIE (Laboratory Reagent and Fine Chemicals), Mumbai, India, of 98 percent purity with CAS number 10196-18-6.

Synthesis of ZnO NPs from *E. coli and A. niger* (bacterial and fungal strain):
Initially, 25 mL of culture was extracted and diluted with 75 mL of sterile distilled water supplemented with nutrition broth for bacteria and potato dextrose broth for fungi. The diluted culture fluid was subsequently incubated for an additional 24 hours for bacteria and 72 hours for fungi. Subsequently, 100 mg of zinc nitrate hexahydrate (final concentration 3.36 mM) was introduced to the cultures of *E. coli and A. niger*, which were incubated at 37°C for 24 hours and 30°C for 72 hours, respectively, until white precipitate formed at the bottom of the conical flask, signifying ion transformation. The culture fluid was cooled and incubated at ambient temperature. Following 12–48 hours of incubation on a rotary shaker, the reaction mixture exhibited distinct white precipitates settled at the bottom of the flask. Subsequent to incubation, the broth culture was centrifuged at 5000 rpm for 15 minutes. The supernatant and pellet were isolated and desiccated for subsequent analysis. The supernatant was placed in a watch glass and allowed to evaporate for the formation of solid powder in a hot air oven.

All experiments were performed in triplicate (n = 3) to ensure reproducibility. The results were expressed as mean ± standard deviation, and statistical analysis was performed using one-way ANOVA, with differences considered statistically significant at $p < 0.05$. Control experiments without microbial culture (containing only zinc nitrate solution and growth media) were maintained under the same experimental conditions. All instruments used for characterization were calibrated prior to analysis using standard calibration references to ensure accuracy and reliability of the measurements.

3. Results

1) Synthesis of ZnO NPs from *E. coli* and *A. niger*:
ZnO NPs were successfully synthesized from *E. coli* and *A. niger*, using zinc nitrate hexahydrate as the precursor. Nanoparticles were synthesized and both supernatant and pellets were analyzed for ZnO NPs formation and analyzed through UV-Vis spectroscopy, FTIR, FE-SEM and antibacterial test. Figure 1, illustrates the microbial development of *E. coli* and *A. niger* in their separate cultures maintained under sterile conditions (a) and (b) respectively. The emergence of turbidity signifies the proliferation of the corresponding species.

Figure 1 (a) and (b), illustrates the growth stage of the cultured *E. coli* and *S. aureus* in nutritional medium at zero hours. The produced cultures of *E. coli* and *S. aureus* were combined with an appropriate concentration of precursor (zinc nitrate hexahydrate) and incubated at room temperature. The mixture was monitored for 24 and 48 hours.

Figure 2, represents the growth stages of *E. coli* and *S. aureus* following a 24-hour incubation period. The mixture is maintained on a rotating shaker (120 rpm) to guarantee uniform air circulation and mixing, hence supporting the growth of bacteria and fungi at appropriate temperatures, ultimately leads to the synthesis of ZnO NPs.

Figure 3 (a) and (b), explains the growth phases of *E. coli* and

S. aureus in a nutritional medium following a 24 hours and 48 hours incubation period respectively. The turbidity observed in the *E. coli* bacterial culture and the mycelial growth in the *A. niger* medium indicate successful nanoparticle synthesis.

Consequently, an effective production of ZnO NPs is achieved utilizing *E. coli* and *A. niger* species. The off-white powder indicates effective synthesis via both intracellular and extracellular routes, in pellet and supernatant forms, as illustrated in Figures 4 (a) and (b) respectively. The synthesis of ZnO NPs is validated by multiple analytical characterization techniques, including UV-Vis spectroscopy, FTIR, FESEM, EDAX, and antibacterial activity assessment.

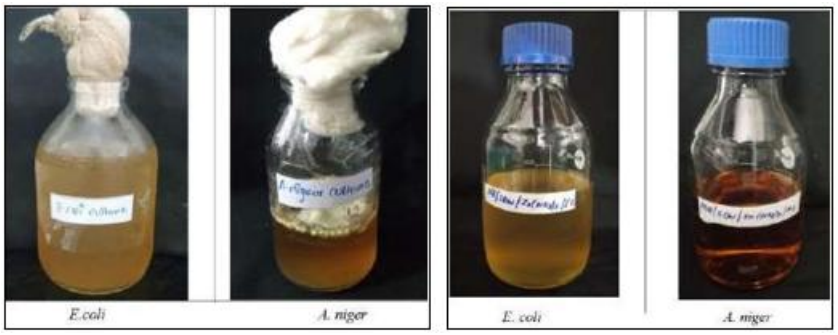

(a) **(b)**

Figure 1: (a) Comparative microbial growth of *E. coli* and *A. niger* cultured under sterile conditions utilized for the synthesis of ZnO NPs, (b) Growth stage of *E. coli* and *A. niger* in nutrient growth medium at zero hours for the synthesis of ZnO NPs

Figure 2: *E. coli* and *A. niger* cultures after 24 hours of incubation period using a rotary shaker

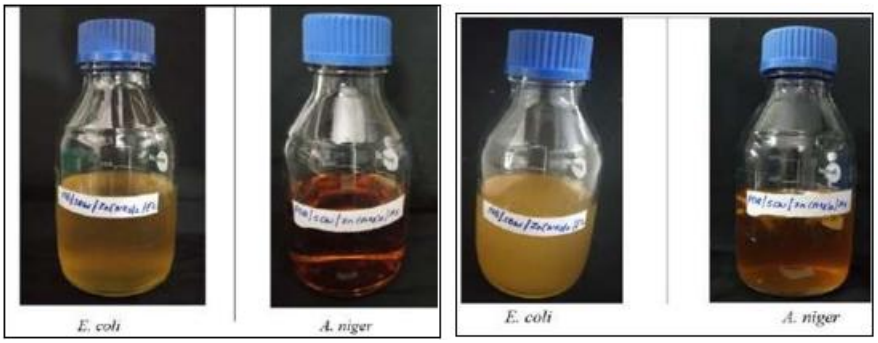

(a) **(b)**

Figure 3: (a) Growth stage of *E. coli* and *A. niger* in nutrient growth medium after 24 hours for the synthesis of ZnO NPs; (b) Growth stage of *E. coli* and *A. niger* in nutrient growth medium after 48 hours for the synthesis of ZnO NPs

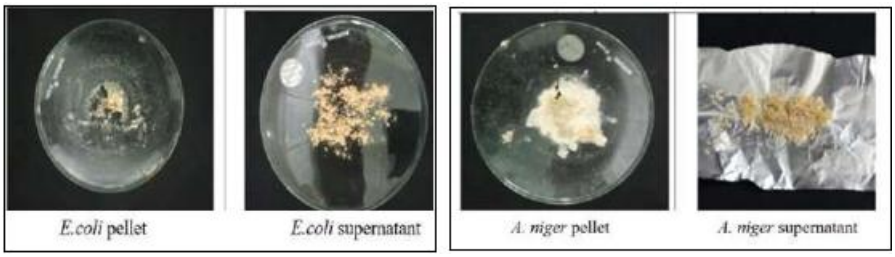

(a) **(b)**

Figure 4: (a) ZnO NPs synthesized using *E. coli* cultures through both, intracellular mechanism (pellet form) and extracellular mechanism (supernatant form) after 48 hours of incubation period; **(b)** ZnO NPs synthesized using *A. niger* cultures through both, intracellular mechanism (pellet form) and extracellular mechanism (supernatant form) after 48 hours of incubation period

Characterization of ZnO NPs using various analytical techniques:

The broth solutions of *E. coli* and *A. niger* were centrifuged at 14,000 to 15,000 rpm for 20 to 25 minutes. The pellets and supernatants were then isolated. The pellets were rinsed with distilled water to eliminate impurities and subsequently dried in an electric oven at 30–35°C to remove moisture while preserving nanoparticles' stability. The produced ZnO NPs were analysed using the following hyphenated analytical methods. The desiccated pellets were preserved in tightly sealed containers for subsequent use. The supernatants were filtered using a 0.22 µm syringe filter to exclude impurities while retaining nanoparticles in the solution. The supernatant was subjected to further centrifugation, washing, and filtering if material was found, until a clear solution was achieved. The supernatant was subsequently evaporated in an oven at 30–35°C until a powdery consistency was achieved. Subsequently, the ZnO NPs from the supernatant were prepared for analysis by diluting 0.01 mL in 5– 7 mL of double-distilled water. In contrast, 0.01 g of ZnO NPs pellets were dispersed in double-distilled water, filtered through a 0.45 µm syringe filter, and both suspensions were subjected to ultrasonication for 30 minutes prior to spectral analysis[16].

A) Ultraviolet-Visible Spectroscopy (UV-Vis Spectroscopy):

The UV-Vis spectra of the produced ZnO NPs were obtained using a Shimadzu Pharmaspec UV-1700 UV-Vis spectrophotometer within the 200-700 nm range. The biosynthesized ZnO NPs were initially evaluated using UV-Vis spectroscopy. The produced ZnO NPs (supernatant and pellets) underwent UV- Vis spectroscopy, confirming the presence of a pronounced peak within the 350-400 nm range[16].

Figures 5(A), reveals UV–Vis spectra of ZnO NPs synthesized using *E. coli* and *A. niger*, respectively, in both pellet and supernatant forms. In Figure 5(A), absorption peaks are observed at 360 nm and 320 nm for (a) and (b), while in Figure 5(B), peaks appear at 310 nm and 315 nm for (a) and (b), respectively. These absorption maxima fall within the expected range of 320–380 nm[16], providing preliminary confirmation of successful ZnO NPs synthesis. The observed variations in peak positions suggest differences in nanoparticle size, shape, and degree of aggregation, which can be attributed to the nature of the capping agents present in the respective broth solutions.

Figure 5(C) illustrates the UV–Vis spectra of the broth solution to validate the synthesis of nanoparticles by the corresponding species. The *E. coli* broth exhibits a UV–Vis spectrum with an absorption peak at 312 nm (a), whereas *A. niger* displays a peak at 311 nm (b). Both peaks are expected to fall within the 320–380 nm range; however, slight shifts are observed, which may be attributed to variations in nanoparticle size, shape, the type of capping agents employed, or nanoparticle aggregation, all of which can influence the spectral range. Figure 5(D) represents UV-Vis spectra of zinc nitrate hexahydrate solution, used as precursor. It shows spectra at 317 nm[17,18], which may be attributed to the presence of zinc ions Zn^{+2} ions.

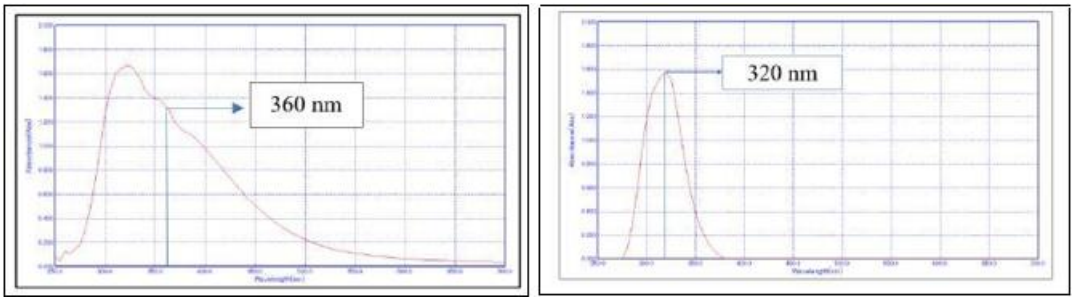

(a) **(b)**

Figure 5 (A): (a) UV-Vis spectra of ZnO NPs synthesized from *E. coli* in the pellet form showing an absorption peak at 360 nm; (b) UV-Vis spectra of ZnO NPs synthesized from *E. coli* in the supernatant form showing an absorption peak at 320 nm

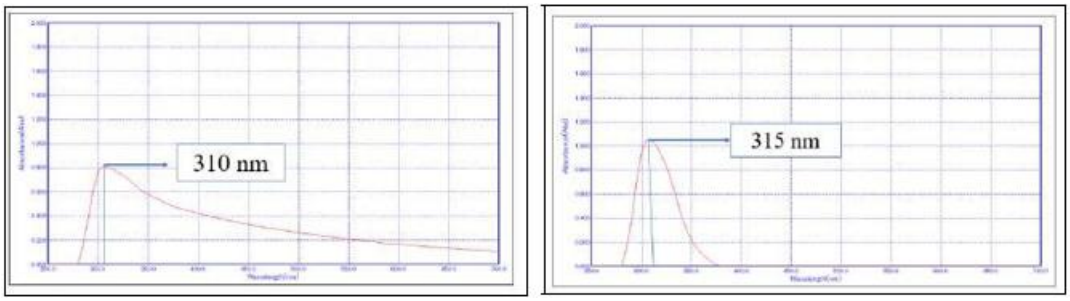

(a) (b)

Figure 5(B): (a) UV-Vis spectra of ZnO NPs synthesized from *A. niger* in the pellet form showing an absorption peak at 310 nm; (b) UV-Vis spectra of ZnO NPs synthesized from *A. niger* in the supernatant form showing an absorption peak at 315nm

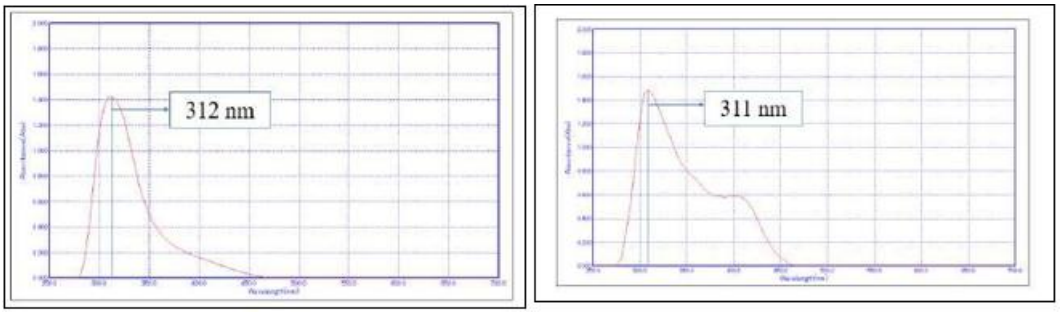

(a) (b)

Figure 5 (C): (a): UV-Vis spectra of *E. coli* broth solution showing an absorption peak at 312 nm; (b) UV-Vis spectra of *A. niger* broth solution showing an absorption peak at 311 nm

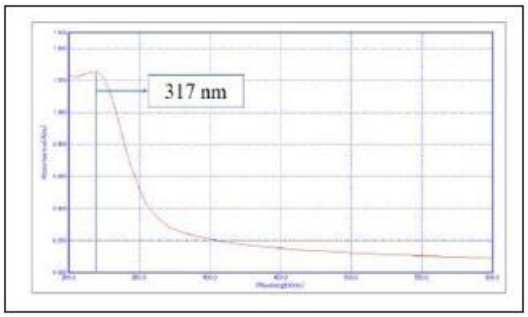

Figure 5 (D): UV-Vis spectra of zinc nitrate hexahydrate solution showing an absorption peak at 317 nm

B) Fourier Transmission Infrared Spectroscopy (FTIR):
The FTIR spectra of the synthesized ZnO NPs using bacteria and fungi for both pellets and supernatant forms were obtained using a Shimadzu IR Prestige-21 spectrophotometer. The detailed peaks are listed in Table 1.

Table 1: List of FTIR data of major peaks corresponding to the samples

S. No.	Samples	Major peaks
1	ZnO NPs from *E. coli* (pellet form)	3442.94cm^{-1}, 1373.32cm^{-1}, 1064.71cm^{-1}, 866.04cm^{-1}, 709cm^{-1} and 646cm^{-1}
2	ZnO NPs from *E. coli* (supernatant form)	3479.58cm^{-1}, 873.75cm^{-1}, 594.08cm^{-1},
3	ZnO NPs from *A. niger* (pellet form)	3437.15cm^{-1}, 1382.03cm^{-1}, 869.90cm^{-1}
4	ZnO NPs from *A. niger* (supernatant form)	3466.48cm^{-1}, 1367.53cm^{-1}, 856.39cm^{-1}, 572.86cm^{-1}
5	*E. coli* broth solution with zinc nitrate hexahydrate	3431.36cm^{-1}, 1381.03cm^{-1}, 1064.00cm^{-1}, 866.04cm^{-1}
6	*A. niger* broth solution with zinc nitrate hexahydrate	3437.15cm^{-1}, 1381.03cm^{-1}, 1051.20cm^{-1}, 869.90cm^{-1}
7	Zinc nitrate hexahydrate solution	3471.87cm^{-1}, 1375.25cm^{-1}, 542.00cm^{-1}

Figure 6, represents a prototype FTIR spectra of ZnO NPs synthesized from *E. coli* in pellet form. The range of 400-800 cm^{-1} corresponds to the stretching vibrations of ZnO NPs, which are missing or exhibit diminished intensity in zinc nitrate solution[23]. The ZnO NPs are effectively synthesized and verified by their presence within the aforementioned range utilizing bacterial and fungal cultures.

FTIR spectra exhibited a significant characteristic peak for ZnO NPs synthesized from *E. coli* and *A. niger* species. Table 1, enumerates the most pronounced, extensive, and strong peaks, highlighting a prevalent peak within the 3400–3600 cm^{-1} range, indicative of hydroxyl groups (OH groups) predominantly adsorbed on the particle surface, likely attributable to ambient moisture[20]. The lower intensity peak within the 1200-1500 cm^{-1} range is attributed to nitrate absorption in zinc nitrate hexahydrate solution, while for other instances, it corresponds to aliphatic C-H bending vibrations. The band between 1000 and 1500 cm^{-1} corresponds to C–O or C–N stretching, commonly associated with alcohols, esters, ethers, and amines[21]. 700-900 cm^{-1} corresponds to metal-oxygen vibrational modes. The peak in commercial ZnO is typically broad due to particle aggregation, while the peak for biosynthesized ZnO is sharp, signifying enhanced crystallinity

and potential size reduction, usually ascribed to the capping and stabilizing agents derived from plant chemicals during green synthesis[22].

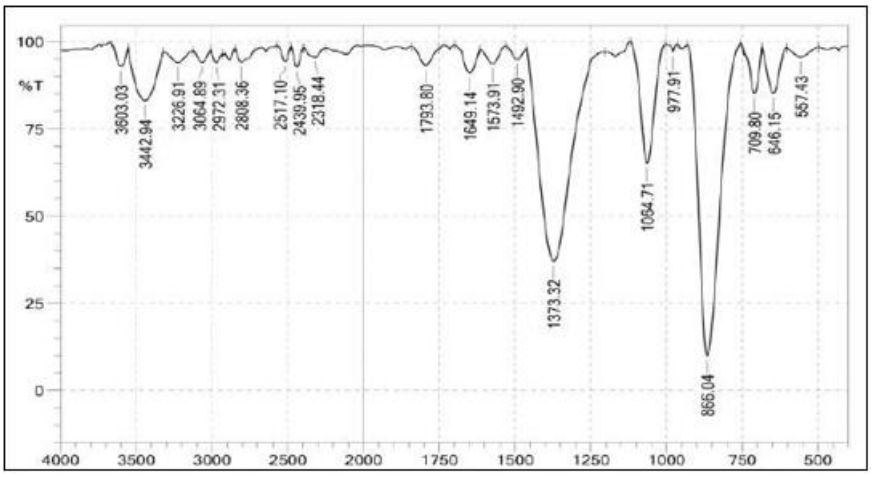

Figure 6: FTIR spectra of ZnO NPs synthesized from *E. coli* in the pellet form

C) Energy Dispersive X-ray Spectroscopy (EDAX):

EDAX analysis is conducted utilizing the Quanta 200 Environmental Scanning Electron Microscope (ESEM). This sophisticated SEM features numerous detectors and an integrated Energy Dispersive X- ray Spectroscopy (EDS) system, providing a resolution of 136 eV for accurate elemental identification and semi-quantitative analysis. EDAX reveals the presence of elements such as oxygen, sodium, potassium, zinc, calcium, and small quantities of additional elements. The maximum Zn content percentage (1.0% wt) is observed in ZnO NPs generated from *A. niger* in the supernatant, whereas the minimum is noted in the other three samples as detailed in Table 2 and Figure 7.

Table 2: EDAX analysis showing percentage weight of zinc along with other elements for various forms of synthesized ZnO NPs

ZnO NPs form	% Weight of zinc	% Weight of other elements present
ZnO NPs from *E. coli* (pellet form)	0.7%	N (9.3%), O (53.1%), Na (19.3%), Mg (1.2%), Ca(15.3%), and Cu (0.6%)
ZnO NPs from *E. coli* (supernatant form)	0.7%	N (8.4%), O (47.1%), Na (38%), Si (0.6%), K(0.3%), and Ca (2.9%)
ZnO NPs from *A. niger* (pellet form)	0.7%	N (13.1), O (52.2), Na (22%), and Ca (11.1),
ZnO NPs from *A. niger* (supernatant form)	1.0%	O (54.9%), Na (36%), Si (0.6%), Ca (7.1%)

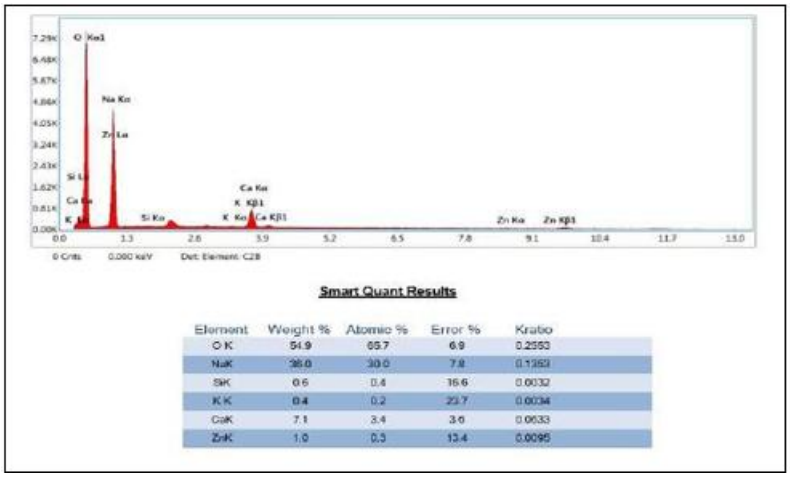

Figure 7: EDAX analysis of ZnO NPs synthesized from *A. niger* in supernatant form, indicating the highest percentage weight of zinc content compared to the other three samples

D) Field Emission Scanning Electron Microscopy (FESEM):

The current research utilized a JEOL JSM IT 200 LV model FESEM instrument for imaging applications. Figure 8 (a–d) displays FESEM images depicting magnified areas of the produced ZnO NPs, with magnifications ranging from 5,000X to 200,000X. ZnO NPs formed with *E. coli* (in both pellet and supernatant forms) displayed flat, sheet-like, spherical, or hexagonal morphologies (Figure 8a), with partial agglomeration noted in certain areas (Figure 8b). Conversely, ZnO NPs formed via *A. niger* (in both pellet and supernatant forms) exhibited primarily spherical morphologies (Figure 8c) with rod-shaped or elongated sheet-like structures (Figure 8d). These observations validate that the selection of biological precursors greatly affects the form and aggregation behaviour of ZnO NPs.

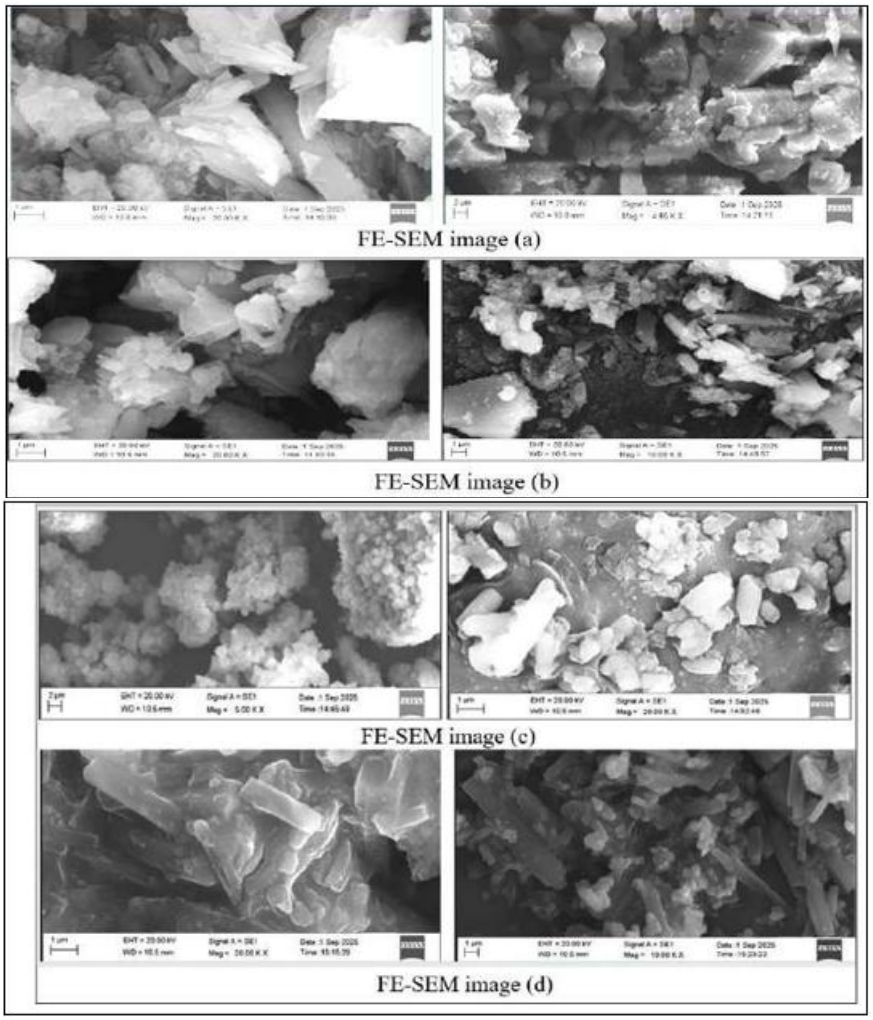

Figure 8: FESEM images of ZnO NPs synthesized using *E. coli* in (a) pellet form and (b) supernatant form and ZnO NPs derived from *A. niger* in (c) pellet form and (d) supernatant form

E) Antibacterial test:

The antibacterial efficacy of biosynthesized ZnO NPs was evaluated against *E. coli* and *S. aureus* strains. The maximum inhibition zone of 17 mm for *E. coli* was recorded at a concentration of 100 µL for ZnO NPs synthesized from *E. coli* (pellet form), followed by 15 mm for ZnO NPs synthesized from *A. niger* (pellet form), and 13 mm for ZnO NPs synthesized from *E. coli* (supernatant form), as illustrated in Figure 9A (a), (b), Figure 9B (a), (b) and Table 3.

The maximum inhibitory zone for *S. aureus* was 18 mm, achieved with ZnO NPs generated from *A. niger* (supernatant form) at a concentration of 100 µL, and 13 mm at 50 µL. Subsequently, ZnO NPs produced from *E. coli* (pellet form) demonstrated inhibitory zones of 17 mm and 14 mm at volumes of 100 µL and 50 µL, respectively as shown in Figure 9C (a), (b), Figure 9D (a), (b) and Table 4.

In contrast, the antibiotic control (gentamicin) demonstrated a 17 mm inhibition against *S. aureus* and a 14 mm inhibition against *E. coli*, while the solvent control (DMSO) displayed no inhibitory effect on either strain, as illustrated in Figure 9E (a), (b) and Table 5.

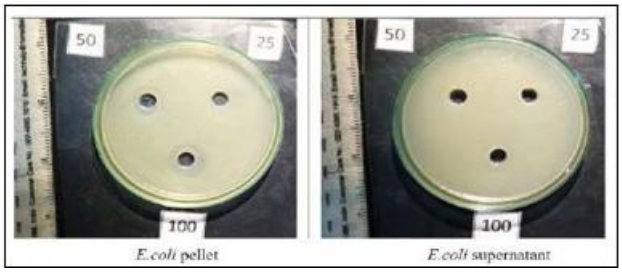

(a) **(b)**

Figure 9(A): Antibacterial effect of ZnO NPs synthesized from *E. coli* bacteria in pellet form (a) and *E. coli* supernatant form (b) against *E. coli* strain, evaluated using the disc diffusion assay.

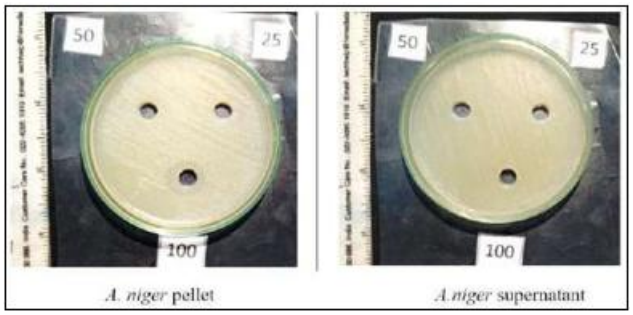

(a) **(b)**

Figure 9(B): Antibacterial effect of ZnO NPs synthesized from *A. niger* fungi in pellet form (a) and supernatant form (b), on *E. coli* strain using disc diffusion assay

Table 3: Zone of inhibition for bacteria (*E. coli*) and fungi (*A. niger*) mediated synthesized ZnO NPs on *E. coli* strain

Zone of inhibition in mm			
Organisms	25µl	50µl	100µl
ZnO NPs *(E. coli)* pellet on *E. coli* strain	NIL	15	17
ZnO NPs *(E. coli)* supernatant on *E. coli* strain	NIL	NIL	13
ZnO NPs (*A. niger*) pellet on *E. coli* strain	NIL	NIL	15
ZnO NPs (*A. niger*) supernatant on *E. coli* strain	NIL	NIL	NIL

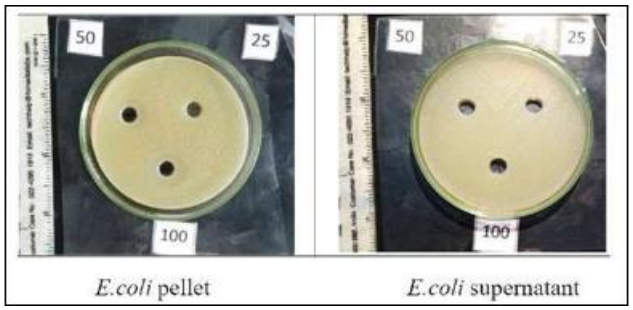

(a) **(b)**

Figure 9(C): Antibacterial effect of ZnO NPs synthesized from *E. coli* bacteria on *S. aureus* strain in pellet form (a) and supernatant form (b), using disc diffusion assay

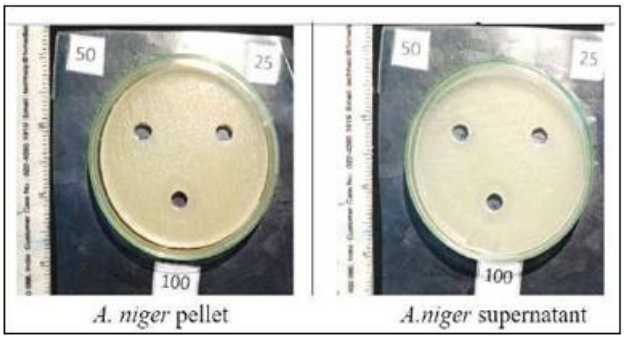

(a) **(b)**

Figure 9 (D): Antibacterial effect of ZnO NPs synthesized from *A. niger* fungi in pellet form (a) and supernatant form (b) on *S. aureus* strain using disc diffusion assay

Table 4: Zone of inhibition for bacteria (*E. coli*) and fungi (*A. niger*) mediated synthesized ZnO NPs on *S. aureus* strain

Zone of inhibition in mm			
Organisms	25µl	50µl	100µl
ZnO NPs *(E. coli)* pellet on *S. aureus* strain	NIL	14	17
ZnO NPs *(E. coli)* supernatant on *S. aureus* strain	NIL	NIL	NIL
ZnO NPs (*A. niger*) pellet on *S. aureus* strain	NIL	NIL	15
ZnO NPs (*A. niger*) supernatant on *S. aureus* strain	NIL	13	18

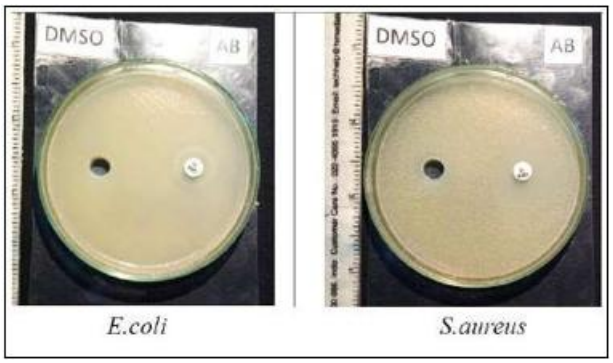

(a) **(b)**

Figure 9 (E): Antibacterial effect of control samples (Gentamicin) on *E. coli* (a) and *S. aureus* strain (b) through disc diffusion method

Table 5: Zone of inhibition for control sample on *E. coli* and *S. aureus* using DMSO and antibiotic (Gentamicin)

Zone of inhibition in mm		
Control	DMSO	AB (antibiotic)
E. coli	NIL	14
S. Aureus	NIL	17

Discussion

ZnO NPs were successfully synthesized using *Escherichia coli (E. coli)* and *Staphylococcus aureus (S. aureus)* through a 48-hour incubation using both extracellular (supernatant-mediated) and intracellular (pellet-mediated) pathways. Post-incubation, both fractions were characterized to confirm ZnO NPs formation, the morphology and antibacterial activity of the synthesized nanoparticles were evaluated. Both microbial species secrete extracellular polymeric substances (EPS) that facilitate nanoparticle reduction, capping, and stabilization, thereby preventing aggregation and maintaining nanoscale dimensions and colloidal stability[12,13].

Nanoparticle synthesis is strongly influenced by parameters such as pH, temperature, metal ion concentration, and incubation time[13]. UV–Vis spectroscopy confirmed ZnO NPs formation, showing characteristic absorbance peaks in the range of 350–400 nm. FE-SEM, EDAX, and XRD analyses provided insights into nanoparticle morphology, elemental composition, crystallinity, and average size. Antibacterial efficacy against *E. coli* and *S. aureus* was evaluated using zone-of-inhibition assays. However, variations in synthesis conditions may affect nanoparticle stability, aggregation behaviour, and surface chemistry, which can indirectly influence antimicrobial performance[13].

The study further demonstrated the potential of *E. coli* bacteria and *A. niger* fungi to synthesize ZnO NPs via a rapid, simple,

and environmentally sustainable biological route without the use of hazardous chemical reducing agents[12]. This green synthesis approach reduces ecological toxicity and offers scalability for industrial production. Optimization of synthesis parameters remains essential to control nanoparticle size and morphology for targeted applications. Differences in nanoparticle characteristics may arise from strain-specific biomolecules acting as capping agents[4]. Key strengths of this approach include environmental sustainability, strain-specific optimization, and comprehensive physicochemical characterization[13]. Future studies will focus on synthesis stability and biological activities such as antibacterial, antioxidant, anti-inflammatory, and catalytic properties [13-15], supporting potential industrial and environmental applications.

UV–Vis analysis revealed absorption peaks within the expected range for ZnO NPs[16-18], with minor peak shifts among samples (360 nm for *E. coli* pellet, 320 nm for *E. coli* supernatant, 310 nm for *A. niger* pellet, and 315 nm for *A. niger* supernatant), indicating variations in particle size, shape, and surface capping. Broth controls showed peaks near 311nm–312 nm, mostly due to biomolecules involved in reduction and stabilization[19-23]. FTIR analysis confirmed the presence of Zn–O stretching vibrations and functional groups associated with ZnO NPs[24], validating nanoparticle synthesis in both bacterial and fungal systems. EDAX results showed the highest zinc weight percentage in *A. niger* derived nanoparticles, highlighting its superior extracellular synthesis capability and suitability for large-scale production[24].

FE-SEM imaging revealed spherical, rod-like, and mildly agglomerated ZnO NPs, indicating effective stabilization. Antibacterial assays demonstrated the largest zones of inhibition for ZnO NPs synthesized using *A. niger* supernatant, consistent with EDAX findings and confirming the superiority of extracellular synthesis over intracellular methods. Future work will incorporate XRD, high-resolution TEM, and DSC to further validate nanoparticle size, crystallinity, and thermal properties[24].

Although the precise mechanism of ZnO NPs biosynthesis remains unclear, extracellular synthesis is simpler and more efficient than intracellular routes[25], as extracellular enzymes and proteins facilitate metal ion reduction and stabilization. Compared to bacteria, fungi generally require longer growth periods but often yield higher nanoparticle productivity[25]. Overall, this study confirms that bacterial and fungal systems can effectively produce ZnO NPs under controlled conditions, offering a viable alternative to plant-mediated synthesis. These biosynthesized nanoparticles show strong potential for applications in biomedical and agricultural sectors.

Conclusion

This study demonstrates a simple and efficient biological route for the synthesis of ZnO NPs using fungal and bacterial systems. UV–V is spectroscopy confirmed nanoparticle formation within the characteristic absorption range of 310 nm –360 nm. FTIR analysis identified hydroxyl, amine, and carbonyl functional groups, which acted as natural reducing, capping, and stabilizing agents during the synthesis process. FE-SEM analysis revealed diverse nanoparticle morphologies, including spherical, rod-like, and hexagonal structures, while EDAX confirmed the elemental presence of zinc. Among the synthesized samples, ZnO NPs derived from *Aspergillus niger* supernatant exhibited the highest zinc content. Antimicrobial evaluation demonstrated a clear concentration-dependent response, with *A. niger* derived ZnO NPs producing larger inhibition zones at higher concentrations compared to other samples. These results indicate that the synthesis pathway and the nature of microbial metabolites play a critical role in determining the physicochemical characteristics and antibacterial efficacy of the nanoparticles. Overall, fungi and bacteria mediated synthesis emerges as an eco-friendly, cost-effective, and sustainable alternative to conventional chemical methods, yielding ZnO NPs with promising biological and functional properties.

Furthermore, the study highlights both intracellular and extracellular synthesis mechanisms employing *E. coli* and *A. niger*, which inherently possess biomolecules capable of converting zinc salts into ZnO NPs. The use of diverse microorganisms provides a versatile platform for tailoring nanoparticle properties through controlled optimization of parameters such as precursor concentration, microbial strain, pH, temperature, incubation conditions, and nutrient media. Such microbial approaches not only reduce environmental burden but also enable scalable and application-specific nanoparticle production, highlighting the effectiveness of microbial systems as sustainable and eco-friendly alternatives to conventional synthesis methods. As research progresses, further optimization of synthesis parameters can enhance nanoparticle properties for targeted biomedical, environmental, and industrial applications, increasing the relevance of biogenic ZnO NPs in these fields.

Acknowledgement
The authors gratefully acknowledge the Chemistry Department and the Microbiology Department of Ramnarain Ruia Autonomous College, Mumbai, for their invaluable support in conducting the synthesis and analysis work.

Conflict of Interest
The authors hereby declare that no conflict of interest exist among themselves.

References

[1] Gunalan, S., Sivaraj, R., Rajendran, V. Green synthesized ZnO nanoparticles against bacterial and fungal pathogens. *Progress in Natural Science: Materials International*, 22(6), 693–700 (2012).
[2] Pantidos, N. Biological synthesis of metallic nanoparticles by bacteria, fungi and plants. *Journal of Nanomedicine & Nanotechnology*, 5(5) (2014).
[3] Bahrulolum, H., Nooraei, S., Javanshir, N., Tarrahimofrad, H., Mirbagheri, V. S., Easton, A. J., et al. Green synthesis of metal nanoparticles using microorganisms and their application in the agrifood sector. *Journal of Nanobiotechnology*, 19(1) (2021).
[4] Yusof, H. M., Mohamad, R., Zaidan, U. H., Rahman, N. A. A. Microbial synthesis of zinc oxide nanoparticles and their potential application as an antimicrobial agent. *Journal of Animal Science and Biotechnology*, 10(1) (2019).

[5] Murali, M., Gowtham, H. G., Shilpa, N., Singh, S. B., Aiyaz, M., Sayyed, R. Z., et al. Nanobiotechnology approaches for sustainable agriculture and food systems. *Frontiers in Microbiology*, 14, 1227951 (2023).
[6] Sikkander, A. M., Bassyouni, F., Yasmeen, K., Mishra, S. R., Lakshmi, V. V. Biogenic synthesis of metal nanoparticles and their environmental applications. *Applied Organometallic Chemistry*, 3(4), 255–267 (2023).
[7] Iravani, S. Green synthesis of metal nanoparticles using plants. *ISRN Nanotechnology* (2014).
[8] Slavin, Y. N., Asnis, J., Häfeli, U. O., Bach, H. Metal nanoparticles: understanding the mechanisms behind antibacterial activity. *Journal of Nanobiotechnology*, 15(1) (2017).
[9] Selvarajan, E., Mohanasrinivasan, V. Biosynthesis and characterization of ZnO nanoparticles using Lactobacillus plantarum. *Materials Letters*, 112, 180–182 (2013).
[10] Mishra, D. N., Prasad, L., Suyal, U. Microbial synthesis of zinc oxide nanoparticles and their biomedical applications. *Frontiers in Microbiology*, 16 (2025).
[11] Sidhu, A. K., Agrawal, S. B., Verma, N., Kaushal, P., Sharma, M. Green synthesis of nanoparticles and their applications in nanotechnology. *Frontiers in Nanotechnology*, 7 (2025).
[12] Rauf, M. A., Owais, M., Rajpoot, R., Ahmad, F., Khan, N., Zubair, S. Biogenic synthesis of ZnO nanoparticles and their antimicrobial activity. *RSC Advances*, 7(58), 36361–36373 (2017).
[13] Ouf, M. S. M., Duab, M. E. A., Abdel-Meguid, D. I., El-Sharouny, E. E., Soliman, N. A. Green synthesis of zinc oxide nanoparticles using microorganisms and their antimicrobial activity. *Microbial Cell Factories*, 24(1) (2025).
[14] Navale, G. R., Late, D. J., Shinde, S. S. Biosynthesis of ZnO nanoparticles using microorganisms. *Journal of Scientific and Medical Central* (2015).
[15] Hemdan, B. A., El-Naggar, M. E., Abd-Elgawad, S. E., Zawawy, N. A. E., Mahmoud, Y. A.-G. Green synthesis of metal nanoparticles using biological systems and their applications. *Biomass Conversion and Biorefinery*, 14(19), 23381–23394 (2023).
[16] Jayaseelan, C., Rahuman, A. A., Kirthi, A. V., Marimuthu, S., Santhoshkumar, T., Bagavan, A., et al. Novel microbial route to synthesize ZnO nanoparticles and their antibacterial activity. *Spectrochimica Acta Part A: Molecular and Biomolecular Spectroscopy*, 90, 78–84 (2012).
[17] Nawaz, H. R., Solangi, B. A., Zehra, B., Nadeem, N. Synthesis and characterization of ZnO nanoparticles by biological method. *Canadian Journal of Scientific and Industrial Research*, 2(4), 164–170 (2011).
[18] Kempegowda, R. G., Gokavi, R. B., Murthy, K. R. S., Banks, C. E. Green synthesis of ZnO nanoparticles and their applications. *Journal of Mines, Metals and Fuels*, 43–51 (2023).
[19] Das, R. P., Pradhan, A. K. Zinc oxide nanomaterials: synthesis and applications. *Springer eBook* (2021).
[20] Gan, F., Wu, K., Ma, F., Du, C. Biosynthesis of metal nanoparticles and their applications. *Molecules*, 25(24), 5838 (2020).
[21] Ramesh, M., Anbuvannan, M., Viruthagiri, G. Green synthesis of ZnO nanoparticles using plant extract and their antibacterial activity. *Spectrochimica Acta Part A: Molecular and Biomolecular Spectroscopy*, 136, 864–870 (2014).
[22] Alamdari, S., Ghamsari, M. S., Lee, C., Han, W., Park, H.-H., Tafreshi, M. J., et al. Green synthesis of ZnO nanoparticles using plant extracts. *Applied Sciences*, 10(10), 3620 (2020).
[23] Djearamane, S., Xiu, L.-J., Wong, L.-S., Rajamani, R., Bharathi, D., Kayarohanam, S., et al. Green synthesis of ZnO nanoparticles and their coating applications. *Coatings*, 12(12), 1864 (2022).
[24] Yusof, H. M., Rahman, N. A., Mohamad, R., Zaidan, U. H., Samsudin, A. A. Microbial synthesis of zinc oxide nanoparticles and their antibacterial activity. *Scientific Reports*, 10(1) (2020).
[25] Murali, M., Gowtham, H. G., Shilpa, N., et al. Microbial nanotechnology for sustainable agriculture and environmental applications. *Frontiers in Microbiology* (2023).